mathematics

Article

Dynamical Analysis of a One- and Two-Scroll Chaotic System

Meng Liu [1], Zhaoyan Wu [2,3,*] and Xinchu Fu [4]

[1] Jiaxing Nanyang Polytechnic Institute, Jiaxing 314003, China
[2] School of Mathematics and Statistic, Jiangxi Normal University, Nanchang 330022, China
[3] Jiangxi Provincial Center of Applied Mathematics, Jiangxi Normal University, Nanchang 330022, China
[4] Department of Mathematics, Shanghai University, Shanghai 200072, China
* Correspondence: zhywu@jxnu.edu.cn; Tel.: +86-791-8812-0367

Abstract: In this paper, a three-dimensional (3D) autonomous chaotic system is introduced and analyzed. In the system, each equation contains a quadratic crossproduct. The system possesses a chaotic attractor with a large chaotic region. Importantly, the system can generate both one- and two-scroll chaotic attractors by choosing appropriate parameters. Some of its basic dynamical properties, such as the Lyapunov exponents, Lyapunov dimension, Poincaré maps, bifurcation diagram, and the chaotic dynamical behavior are studied by adjusting different parameters. Further, an equivalent electronic circuit for the proposed chaotic system is designed according to Kirchhoff's Law, and a corresponding response electronic circuit is also designed for identifying the unknown parameters or monitoring the changes in the system parameters. Moreover, numerical simulations are presented to perform and complement the theoretical results.

Keywords: chaotic system; Lyapunov exponent; bifurcation; electronic circuit; parameter identification

MSC: 34C28

check for updates

Citation: Liu, M.; Wu, Z.; Fu, X. Dynamical Analysis of a One- and Two-Scroll Chaotic System. *Mathematics* **2022**, *10*, 4682. https://doi.org/10.3390/math10244682

Academic Editor: Luigi Fortuna

Received: 19 November 2022
Accepted: 8 December 2022
Published: 9 December 2022

1. Introduction

Since the first discovery of chaotic attractors by Lorenz in 1963 [1], chaos has attracted attention and interest for its useful speciality and application in information and computer science [2]. The proposals of new chaotic systems have been extensively studied by scientists in the past decades. In 1976, Rössler found a new simple 3D quadratic autonomous chaotic system with only one quadratic nonlinearity on the right-hand side [3].

In 1999, Chen found another chaotic attractor [4]. Recently, Lü and Chen further found a new chaotic system, which represented the transition between the Lorenz and the Chen system [5]. Moreover, Liu and Chen introduced a new chaotic system with three quadratic nonlinearities on the right-hand side in 2003 [6], which displayed two- and four-scroll attractors for different parameters. Then, Lü and Chen constructed another simple 3D system, which displayed two chaotic attractors simultaneously [7].

During the past few years, some new 3D chaotic systems have been analyzed [8–20]. To classify these 3D autonomous chaotic systems, Vaněček and Čelikoshý [21] gave a divertive classification by separating the linear and quadratic parts of a 3D autonomous system. The linear part was described by a constant matrix $A = [a_{ij}]_{3\times 3}$. The Lorenz system satisfied $a_{12}a_{21} > 0$, the Chen system satisfied $a_{12}a_{21} < 0$, and the Lü system satisfied $a_{12}a_{21} = 0$. As is known, the Lorenz system and Chen system display a two-scroll chaotic attractor separately. In this paper, we introduce a 3D autonomous system, in which each equation contains a quadratic crossproduct, and the constant matrix of the linear part satisfies $a_{12}a_{21} = 0$. Different from Lorenz-like systems, the proposed system can display different numbers of scroll chaotic attractors simultaneously. The system is described by:

$$\begin{cases} \dot{x} = ay - yz, \\ \dot{y} = -bz + zx, \\ \dot{z} = cx + xy - dz, \end{cases} \tag{1}$$

in which $(x, y, z)^T \in \Re^3$, and a, b, c, and d are real parameters. Though system (1) has three quadratic nonlinearities on the right-hand side, it can display only one-scroll attractor in contrast to the Rössler attractor and Sprott's attractor [22,23]. Simultaneously, with the appropriate parameters, the system (1) can display a two-scroll attractor in contrast to the famous Lorenz attractor. This system is a supplement to the discovery of two-scroll band structure attractors.

Further, according to Kirchhoff's law, we design an equivalent electronic circuit for the proposed chaotic system to show its practical applications. The system parameters of an electronic circuit maybe unknown or uncertain. Thus, based on the parameter identification and adaptive synchronization of drive–response systems, we design a corresponding response electronic circuit to identify the unknown parameters or monitor the changes in the system parameters.

The outline of this paper is as follows. In Section 2, the basic dynamical behavior in the parameter space is discussed, and some parameter examples for generating chaos are given. In Section 3, bifurcation analysis and the simulation results of the chaotic system are presented. In Section 4, a vector map is employed to generalized different attractors with the same parameters in the system. In Section 5, the adaptive synchronization problem between the drive–response systems with fully unknown parameters is studied. Finally, conclusions are drawn in Section 6.

2. Basic Dynamical Behavior of the System

The divergence of system (1) is

$$\nabla\dot{V} = \frac{\partial\dot{x}}{\partial x} + \frac{\partial\dot{y}}{\partial y} + \frac{\partial\dot{z}}{\partial z} = 0 + 0 - d = -d. \tag{2}$$

Therefore, when parameter d is positive, system (1) is dissipative.

The equilibria of system (1) can be obtained by solving the following algebraic equations:

$$ay - yz = 0, \ -bz + xz = 0, \ cx + xy - dz = 0.$$

When $bd \neq 0$, the system has three equilibria:

$$S_1 = (0,0,0)^T, \ S_2 = (b, \frac{ad - bc}{b}, a)^T, \ S_3 = (b, 0, \frac{bc}{d})^T.$$

In addition, under the condition $b = 0$ (or $d = 0$), the system has a unique equilibrium $S_{01}^* = (0,0,0)^T$ (or $S_{02}^* = (b, -c, a)^T$). In the following, we let $b \neq 0$ and $d > 0$. The Jacobian matrix of system (1) at the three equilibria S_1, S_2, and S_3 are

$$J_1 = \begin{pmatrix} 0 & a & 0 \\ 0 & 0 & -b \\ c & 0 & -d \end{pmatrix}, J_2 = \begin{pmatrix} 0 & 0 & \frac{bc-ad}{b} \\ a & 0 & 0 \\ \frac{ad}{b} & b & -d \end{pmatrix},$$

$$J_3 = \begin{pmatrix} 0 & \frac{ad-bc}{d} & 0 \\ \frac{bc}{d} & 0 & 0 \\ c & b & -d \end{pmatrix}.$$

The characteristic equations of J_1, J_2, and J_3 are

$$\lambda^3 + d\lambda^2 + abc = 0, \tag{3}$$

$$\lambda^3 + d\lambda^2 + \frac{a^2d^2 - abcd}{b^2}\lambda + a^2d - abc = 0, \tag{4}$$

$$(\lambda + d)(\lambda^2 + \frac{b^2c^2 - abcd}{d^2}) = 0. \tag{5}$$

Obviously, from Equation (5), the equilibrium S_3 is a saddle for $bc(bc - ad) < 0$ and is a center for $bc(bc - ad) > 0$.

According to the Routh–Hurwitz criterion [24,25], for a cubic characteristic equation

$$\lambda^3 + a_1\lambda^2 + a_2\lambda + a_3 = 0, \tag{6}$$

the real part of the roots of the cubic Equation (6) is negative if and only if $a_1 > 0$, $a_3 > 0$, $a_1a_2 - a_3 > 0$, i.e., (6) satisfies the condition $|arg(\lambda)| > \pi/2$. Then, the equilibrium point of system (1) is locally asymptotically stable.

Comparing Equation (3) with Equation (6), it is impossible to satisfy the conditions $abc > 0$ and $-abc > 0$ simultaneously, i.e., when $abc > 0$ (or $abc < 0$) and $d > 0$, the equilibrium S_1 is unstable. For instance, when $a = 0.4$, $b = 60$, $c = 16$, and $d = 10$, the three eigenvalues corresponding to $S_1 = (0, 0, 0)$ are $\lambda_1 = -12.4696$ and $\lambda_{2,3} = 1.2348 \pm 5.4102i$, and the system has a chaotic attractor at the unstable equilibrium S_1 for the initial value $(0.01, 0.01, 0.01)^T$ as shown in Figure 1.

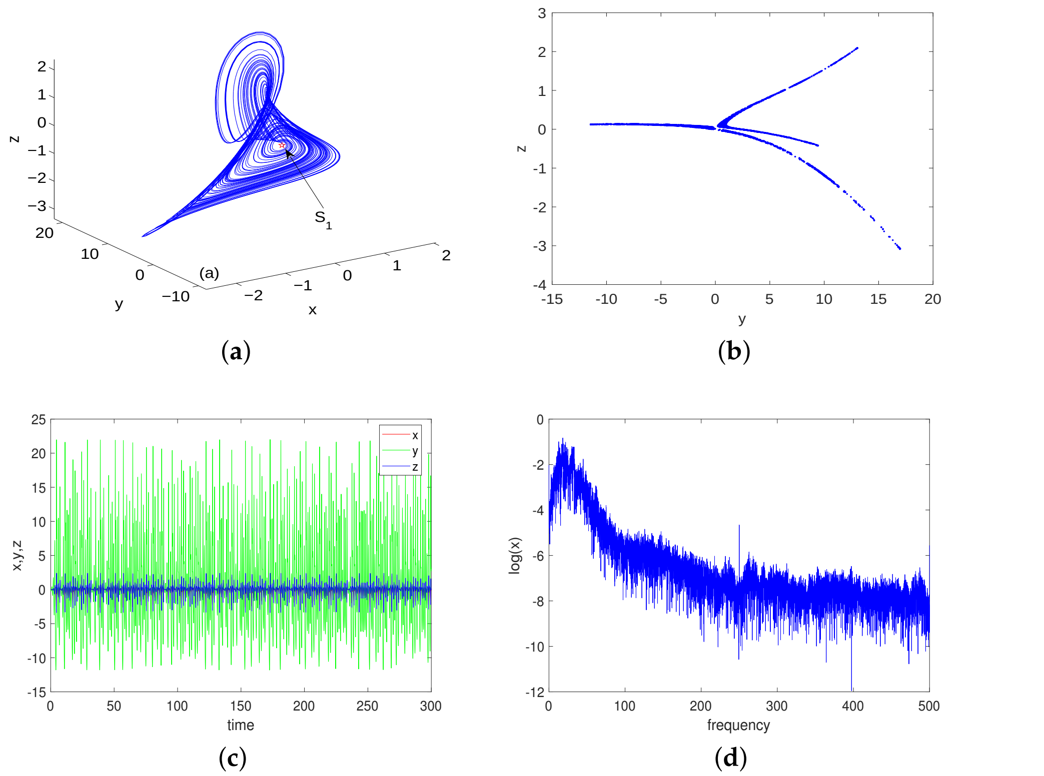

Figure 1. (**a**) Chaotic attractor of system (1) with $(a, b, c, d) = (0.4, 60, 16, 10)$ at the initial values $(0.01, 0.01, 0.01)^T$. (**b**) The corresponding Poincaré map on plane $x = 0$. (**c**) The time series of the x, y, z states. (**d**) The power spectrum of the x state.

Similarly, comparing Equation (4) with Equation (6), when one or two of the three conditions (i.e., $a(ad - bc) > 0$, $d^2 - b^2 > 0$, and $d > 0$) are not satisfied, the equilibrium S_2 is unstable, and system (1) can generate chaos at S_1 and S_2. For instance, when $a = 5$, $b = 50$, $c = -6$, and $d = 13$, the three eigenvalues corresponding to $S_2 = (50, 7.3, 5)^T$ are $\lambda_1 = -18.0662$ and $\lambda_{2,3} = 2.5331 \pm 9.7263i$, and the three eigenvalues corresponding to $S_3 = (50, 0, -23.0769)^T$ are $\lambda_1 = -13$ and $\lambda_{2,3} = \pm 25.4544i$. The system has a chaotic attractor at unstable equilibrium S_2, as shown in Figure 2.

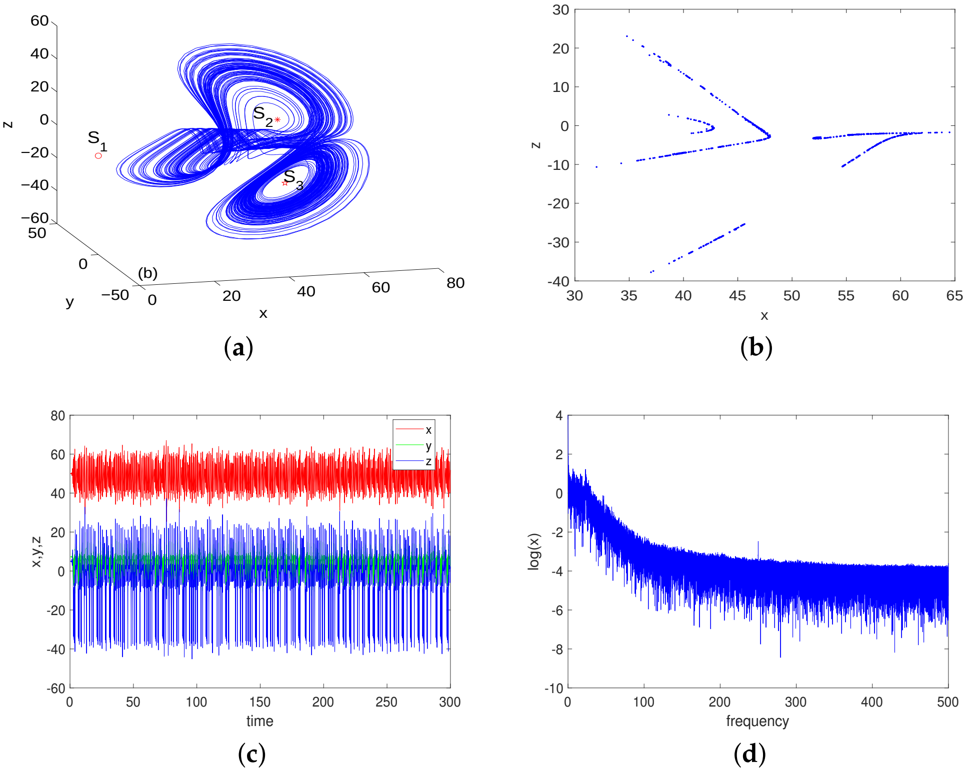

Figure 2. (**a**) Chaotic attractor of system (1) with $(a, b, c, d) = (5, 50, -6, 13)$ at the initial values $(50.01, 7.31, 5.01)^T$. (**b**) The corresponding Poincaré map on plane $y = 5$. (**c**) The time series of the x, y, z states. (**d**) The power spectrum of the x state.

3. Bifurcation Analysis

As is known, for a 3D autonomous system, its three Lyapunov exponents L_1, L_2, and L_3 can be obtained by using the Wolf algorithm [26]. For the equilibrium points, $L_3 < L_2 < L_1 < 0$, for the periodic orbits, $L_3 < L_2 < 0$, $L_1 = 0$, and for the chaotic attractor, $L_3 < 0, L_2 = 0$, $L_1 > 0$. In the following, the Lyapunov exponent spectrum and the corresponding bifurcation diagram of state variable x with respect to different parameters are shown, and the basic dynamics of the chaotic system (1) are summarized as follows. In addition, the Lyapunov exponents L_i and the Lyapunov dimension D_L are listed, in which the Lyapunov dimension of chaos attractors is a fractional dimension, described as:

$$D_L = j + \frac{1}{\mid L_{j+1} \mid} \sum_{i=1}^{j} L_i = 2 + \frac{L_1 + L_2}{\mid L_3 \mid}. \tag{7}$$

In this section, system (1) is investigated under the condition that the four parameters are all positive, as shown in Table 1. Some examples according to different conditions of the parameters are shown in Tables 1 and 2, which cause system (1) to display chaotic attractors at S_1 and S_2, respectively.

Table 1. Parameter examples and Lyapunov exponents for chaotic system (1) that generate chaos at the equilibrium S_1.

$abc > 0$ and $d > 0$	Parameter Examples	Lyapunov Exponents	D_L	Initial Values
$a > 0,\ b > 0,\ c > 0,$	$a = 0.3,\ b = 60,\ c = 16,\ d = 10$	$L_1 = 0.422,\ L_2 = 0,\ L_3 = -10.419$	2.0404	$(0.01, 0.01, 0.01)^T$
	$a = 0.45,\ b = 62,\ c = 16.1,\ d = 9$	$L_1 = 0.883,\ L_2 = 0,\ L_3 = -9.883$	2.0897	$(0.01, 0.01, 0.01)^T$
	$a = 1.2,\ b = 18,\ c = 15,\ d = 8$	$L_1 = 0.776,\ L_2 = 0,\ L_3 = -8.775$	2.0885	$(0.01, 0.01, 0.01)^T$
$a > 0,\ b < 0,\ c < 0,$	$a = 0.85,\ b = -20,\ c = -16,\ d = 10$	$L_1 = 0.314,\ L_2 = 0,\ L_3 = -10.314$	2.0306	$(0.01, 0.01, 0.01)^T$
	$a = 0.85,\ b = -30,\ c = -19,\ d = 1$	$L_1 = 0.895,\ L_2 = 0,\ L_3 = -10.891$	2.0821	$(0.01, 0.01, 0.01)^T$
	$a = 0.65,\ b = -30,\ c = -16,\ d = 10$	$L_1 = 0.443,\ L_2 = 0,\ L_3 = -10.441$	2.0424	$(0.01, 0.01, 0.01)^T$
$a < 0,\ b < 0,\ c > 0,$	$a = -2,\ b = -21,\ c = 16,\ d = 10$	$L_1 = 1.022,\ L_2 = 0,\ L_3 = -11.020$	2.0931	$(0.01, 0.01, 0.01)^T$
	$a = -2,\ b = -15,\ c = 16,\ d = 9$	$L_1 = 0.881,\ L_2 = 0,\ L_3 = -9.882$	2.0896	$(0.01, 0.01, 0.01)^T$
	$a = -10,\ b = -8,\ c = 9,\ d = 8$	$L_1 = 1.115,\ L_2 = 0,\ L_3 = -9.115$	2.1236	$(0.01, 0.01, 0.01)^T$
$a < 0,\ b > 0,\ c < 0,$	$a = -1,\ b = 40,\ c = -18,\ d = 12$	$L_1 = 0.924,\ L_2 = 0,\ L_3 = -12.918$	2.0715	$(0.01, 0.01, 0.01)^T$
	$a = -0.7,\ b = 30,\ c = -16,\ d = 10$	$L_1 = 0.570,\ L_2 = 0,\ L_3 = -10.568$	2.0539	$(0.01, 0.01, 0.01)^T$
	$a = -1.2,\ b = 20,\ c = -16,\ d = 9$	$L_1 = 0.743,\ L_2 = 0,\ L_3 = -9.742$	2.0763	$(0.01, 0.01, 0.01)^T$

Table 2. Parameter examples and Lyapunov exponents for chaotic system (1) that generate chaos at the equilibrium S_1.

$abc < 0$ and $d > 0$	Parameter Examples	Lyapunov Exponents	D_L	Initial Values
$a(ad - bc) > 0,$ $d^2 - b^2 < 0,\ b > 0$	$a = 5,\ b = 50,\ c = -6,\ d = 13$	$L_1 = 1.283,\ L_2 = 0,\ L_3 = -14.261$	2.0906	$(50.01, 7.31, 5.01)^T$
	$a = 12,\ b = 50,\ c = -6.1,\ d = 13$	$L_1 = 1.586,\ L_2 = 0,\ L_3 = -14.574$	2.1093	$(50.01, 7.31, 5.01)^T$
	$a = -16,\ b = 60,\ c = 3,\ d = 9$	$L_1 = 1.328,\ L_2 = 0,\ L_3 = -10.328$	2.1290	$(50.01, 7.31, 5.01)^T$
$a(ad - bc) > 0,$ $d^2 - b^2 < 0,\ b < 0$	$a = 16,\ b = -60,\ c = 3,\ d = 9$	$L_1 = 1.365,\ L_2 = 0,\ L_3 = -10.367$	2.1277	$(-50.01, 7.31, 5.01)^T$
	$a = 10,\ b = -50,\ c = 3,\ d = 10$	$L_1 = 1.376,\ L_2 = 0,\ L_3 = -11.366$	2.1212	$(-50.01, 7.31, 5.01)^T$
	$a = 20,\ b = -70,\ c = 3,\ d = 10$	$L_1 = 1.383,\ L_2 = 0,\ L_3 = -11.379$	2.1216	$(-50.01, 7.31, 5.01)^T$

We fixed $b = 60$, $c = 16$, and $d = 10$, and the Lyapunov exponent spectrum with respect to a is shown in Figure 3. When the parameter a varied in the small interval $(0, 0.66)$, system (1) had very rich dynamical behaviors, i.e., when $a \in (0, 0.171) \cup (0.219, 0.231) \cup (0.257, 0.269) \cup (0.473, 0.526)$, the maximum Lyapunov exponent equaled zero, and system (1) had periodic orbits, and when $a \in (0.171, 0.219) \cup (0.231, 0.257) \cup (0.269, 0.473) \cup (0.526, 0.66)$, there was one positive Lyapunov exponent, and system (1) was chaotic.

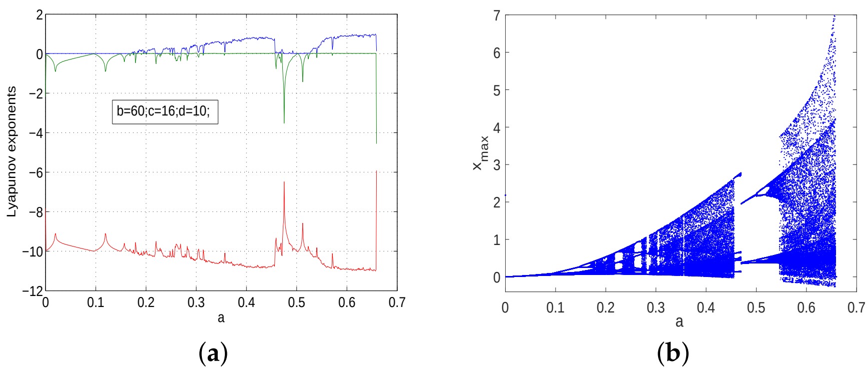

Figure 3. The Lyapunov exponents spectrum and the bifurcation diagram of system (1) with $(b, c, d) = (60, 16, 10)$ and $0 < a < 0.66$ at the initial values $(0.01, 0.01, 0.01)^T$: (**a**) Lyapunov exponents; (**b**) bifurcation diagram.

We fixed a, c, and d, and the Lyapunov exponent spectrum with respect to b is shown in Figures 4 and 5. We fixed $a = 0.4$, $c = 16$, and $d = 10$; when b varied in the interval $(0, 97)$, system (1) had very rich dynamical behaviors at the initial values $(0.01, 0.01, 0.01)^T$, i.e., when $b \in (0, 25.7) \cup (29.3, 30.2) \cup (32.9, 35) \cup (39.3, 41) \cup (68.5, 78.5)$, the maximum Lyapunov exponent equaled zero, and system (1) had periodic orbits, and when $b \in (25.7, 29.3) \cup (30.2, 32.9) \cup (35, 39.3) \cup (41, 68.5) \cup (78.5, 97)$, there was one positive Lyapunov exponent, and system (1) was chaotic. On the other hand, we fixed $a = 5, c = -6$, and $d = 13$; when b varied in the interval $(45, 60)$, system (1) had very rich dynamical behaviors at the initial values $(50.01, 7.31, 5.01)^T$ as well, i.e., when $b \in (45.6, 46.9) \cup (50.3, 50.5) \cup (54.6, 55.2)$, the maximum Lyapunov exponent equaled zero, and system (1) had periodic orbits, and when $b \in (45, 45.6) \cup (46.9, 50.3) \cup (50.5, 54.6) \cup (55.2, 56.82)$, there was one positive Lyapunov exponent, and system (1) was chaotic.

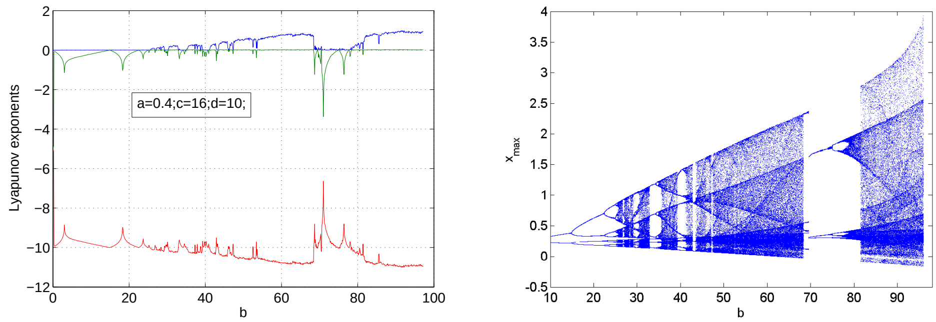

(**a**) (**b**)

Figure 4. The Lyapunov exponents spectrum and the bifurcation diagram of system (1) with $(a, c, d) = (0.4, 16, 10)$ and $0 < b < 97$ at the initial values $(0.01, 0.01, 0.01)^T$: (**a**) Lyapunov exponents; (**b**) bifurcation diagram.

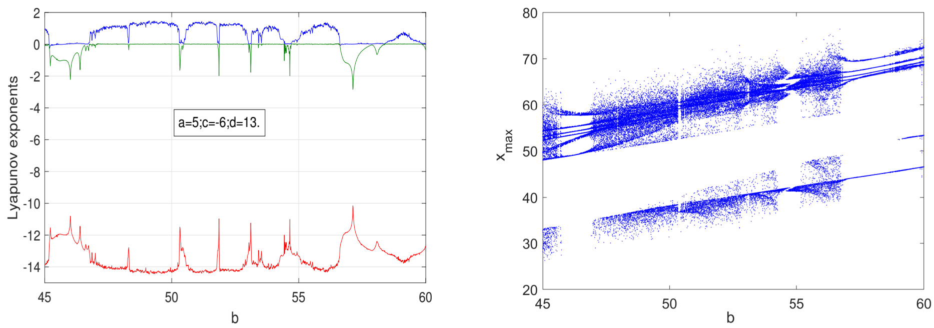

(**a**) (**b**)

Figure 5. The Lyapunov exponents spectrum and the bifurcation diagram of system (1) with $(a, c, d) = (5, -6, 13)$ and $45 < b < 60$ at the initial values $(50.01, 7.31, 5.01)^T$: (**a**) Lyapunov exponents; (**b**) bifurcation diagram.

We fixed $a = 0.4, b = 60$, and $d = 10$; when c varied in the interval $(2.7, 20.2)$, system (1) had very rich dynamical behaviors, i.e., when $c \in (2.7, 9.1) \cup (10.12, 10.21) \cup (11.7, 12.1) \cup (17.38, 17.77)$, the maximum Lyapunov exponent equaled zero, and system (1) had periodic orbits, and when $c \in (9.1, 10.12) \cup (10.21, 11.7) \cup (12.1, 17.38) \cup (17.77, 20.2)$, there was one positive Lyapunov exponent, and system (1) was chaotic. The corresponding Lyapunov exponent and bifurcation diagram are shown in Figure 6.

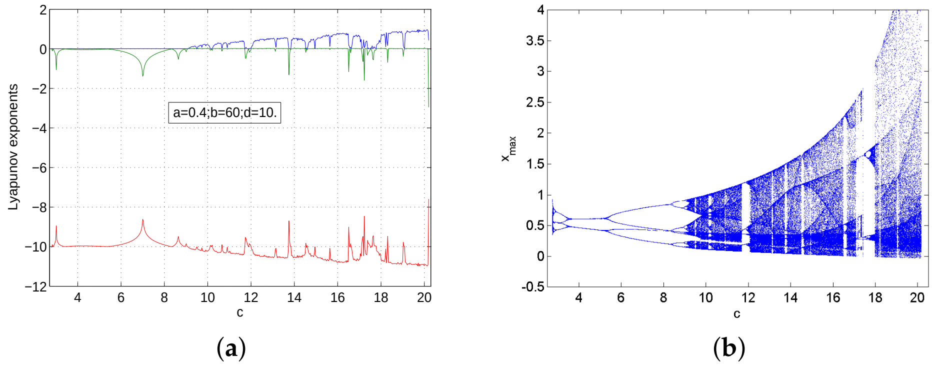

Figure 6. The Lyapunov exponents spectrum and the bifurcation diagram of system (1) with $(a, b, d) = (0.4, 60, 10)$ and $2.7 < c < 20.2$ at the initial values $(0.01, 0.01, 0.01)^T$: (**a**) Lyapunov exponents; (**b**) bifurcation diagram.

We fixed $a = 0.4, b = 60$, and $c = 16$; when d varied in the interval $(8.49, 20)$, system (1) had very rich dynamical behaviors at the initial values $(0.01, 0.01, 0.01)^T$, i.e., when $d \in (9.35, 9.65) \cup (11.58, 20)$, the maximum Lyapunov exponent equaled zero, and system (1) had periodic orbits, and when $d \in (8.49, 9.35) \cup (9.65, 11.58)$, there was one positive Lyapunov exponent. and system (1) was chaotic. The corresponding Lyapunov exponent and bifurcation diagram are shown in Figures 7 and 8. On the other hand, we fixed $a = 5, b = 50$, and $c = -6$; when d varied in the interval $(5, 30)$, system (1) had very rich dynamical behaviors at the initial values $(50.01, 7.31, 5.01)^T$ as well, i.e., when $b \in (5, 5.4) \cup (11.9, 12.2) \cup (13.3, 13.6) \cup (13.8, 14.1) \cup (14.8, 15.1) \cup (16.6, 16.8) \cup (17.8, 23.1) \cup (24.9, 30)$, the maximum Lyapunov exponent equaled zero, and system (1) had periodic orbits, and when $b \in (5.4, 11.9) \cup (12.2, 13.3) \cup (13.6, 13.8) \cup (14.1, 14.9) \cup (15.1, 16.6) \cup (16.8, 17.8) \cup (23.1, 24.9)$, there was one positive Lyapunov exponent, and system (1) was chaotic.

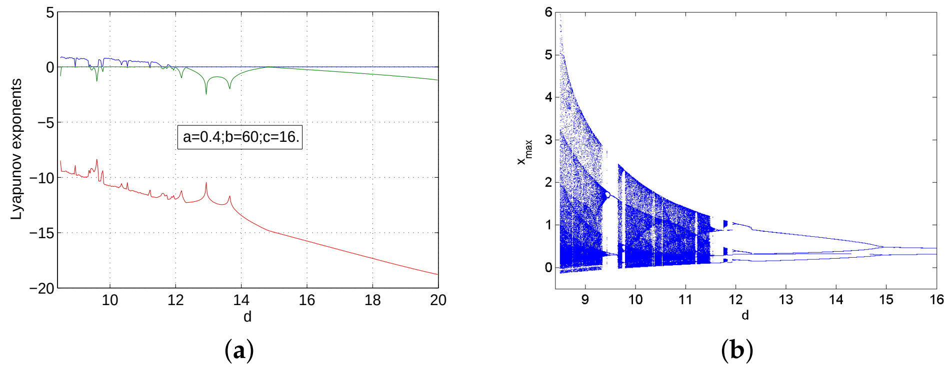

Figure 7. The Lyapunov exponents spectrum and the bifurcation diagram of system (1) with $(a, b, c) = (0.4, 60, 16)$ and $8.49 < d < 20$ at the initial values $(0.01, 0.01, 0.01)^T$: (**a**) Lyapunov exponents; (**b**) bifurcation diagram.

In Figure 9, some simulation results of system (1) with different parameter values are given in the $x - y - z$ space.

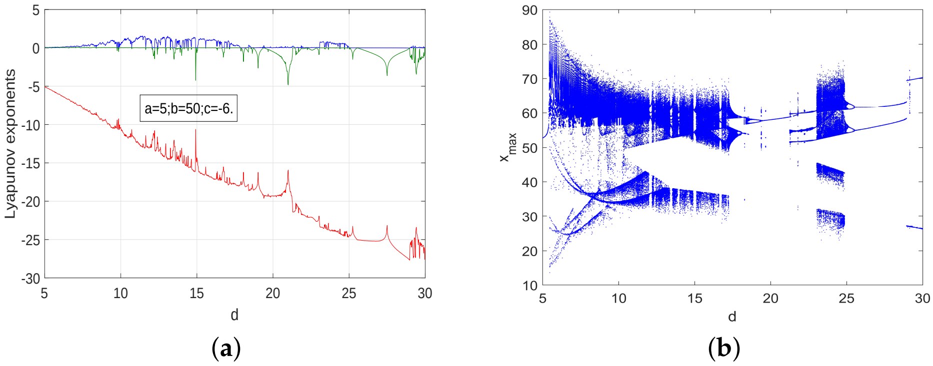

Figure 8. The Lyapunov exponents spectrum and the bifurcation diagram of system (1) with $(a, b, c) = (5, 50, -6)$ and $5 < d < 30$ at the initial values $(50.01, 7.31, 5.01)^T$: (**a**) Lyapunov exponents; (**b**) bifurcation diagram.

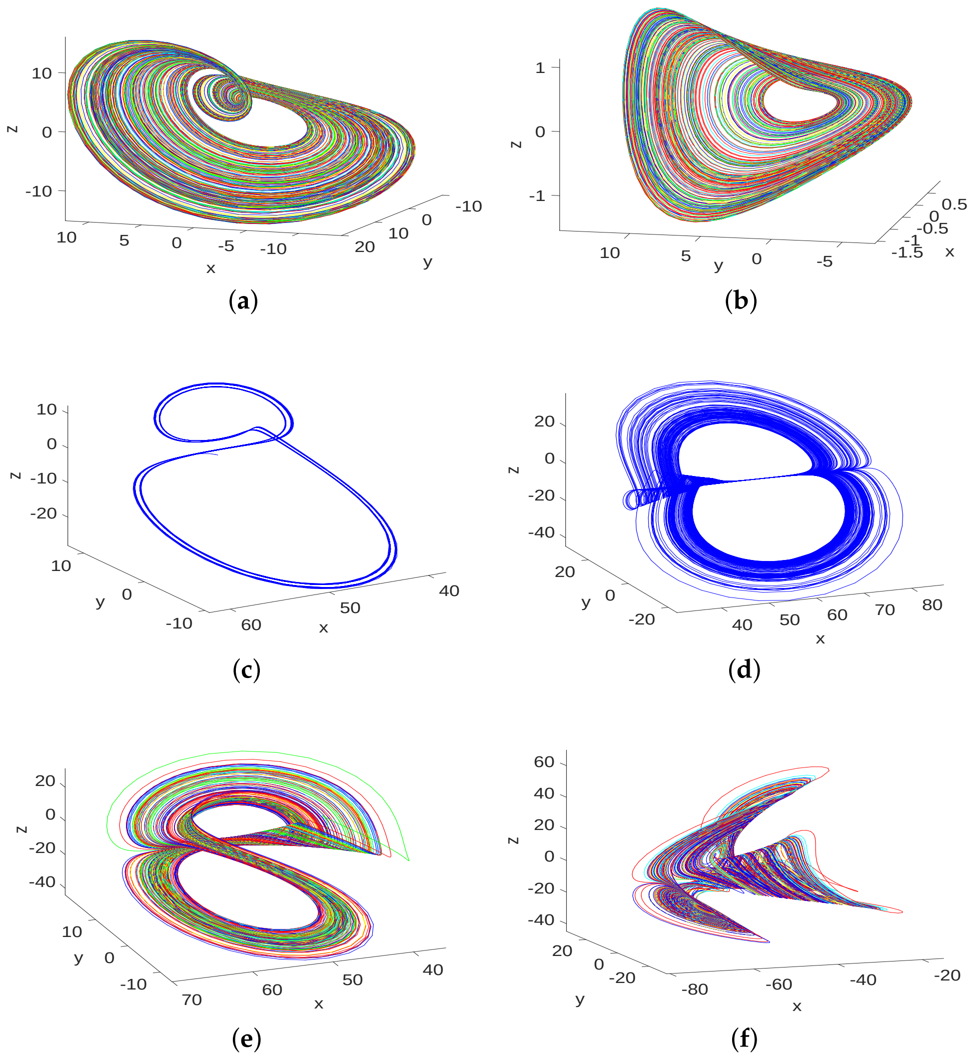

Figure 9. The phase portrait of system (1) with different parameter values: (**a**) $a = 5.8, b = 9, c = 15, d = 11$; (**b**) $a = 0.4, b = 60, c = 10, d = 10$; (**c**) $a = 5, b = 50, c = -6, d = 25.5$; (**d**) $a = 5, b = 60, c = -6, d = 34$; (**e**) $a = 5, b = 55, c = -6, d = 16$; (**f**) $a = 16, b = -60, c = 3, d = 9$.

4. Chaotic Systems Generalized by a Vector Map

In this section, we introduce several chaotic systems generalized by a vector map. Firstly, system (1) can be written as:

$$\begin{pmatrix} \dot{x} \\ \dot{y} \\ \dot{z} \end{pmatrix} = \begin{pmatrix} 0 & y & 0 \\ 0 & 0 & z \\ x & 0 & 0 \end{pmatrix} A + \begin{pmatrix} x & 0 & 0 \\ 0 & y & 0 \\ 0 & 0 & z \end{pmatrix} B + \begin{pmatrix} yz & 0 & 0 \\ 0 & xz & 0 \\ 0 & 0 & xy \end{pmatrix} C, \tag{8}$$

where $A = (c, a, -b)^T$, $B = (0, 0, -d)^T$, and $C = (-1, 1, 1)^T$ are the parameter vectors. Now, we define the following vector maps $\phi_i : \Re^3 \to \Re^3, i = 1, 2:$

$$\begin{aligned} \phi_1((x_1, x_2, x_3)^T) &= (x_2, x_3, x_1)^T, \\ \phi_2((x_1, x_2, x_3)^T) &= (x_3, x_1, x_2)^T. \end{aligned} \tag{9}$$

Then, system (10) is chaotic for the same parameters as (8):

$$\begin{aligned} \begin{pmatrix} \dot{x} \\ \dot{y} \\ \dot{z} \end{pmatrix} = \begin{pmatrix} 0 & y & 0 \\ 0 & 0 & z \\ x & 0 & 0 \end{pmatrix} \phi_i(A) + \begin{pmatrix} x & 0 & 0 \\ 0 & y & 0 \\ 0 & 0 & z \end{pmatrix} \phi_i(B) \\ + \begin{pmatrix} yz & 0 & 0 \\ 0 & xz & 0 \\ 0 & 0 & xy \end{pmatrix} \phi_i(C). \end{aligned} \tag{10}$$

Substituting Equation (9) into (10) yields two chaotic systems (11) and (12) with $a = 1, b = 22, c = 16$, and $d = 10$ and the initial value $(0.1, 0.1, 0.1)^T$. The two chaotic attractors are shown in Figure 10a.

$$\begin{cases} \dot{x} = -by + yz, \\ \dot{y} = cz + zx - dy, \\ \dot{z} = ax - xy, \end{cases} \tag{11}$$

$$\begin{cases} \dot{x} = cy + yz - dx, \\ \dot{y} = az - zx, \\ \dot{z} = -bx + xy. \end{cases} \tag{12}$$

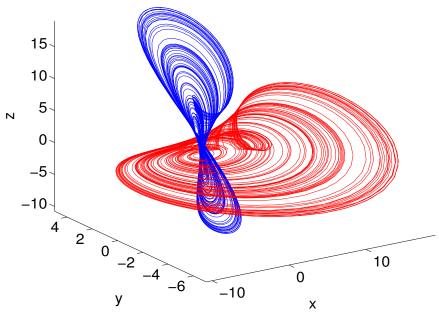

(**a**)

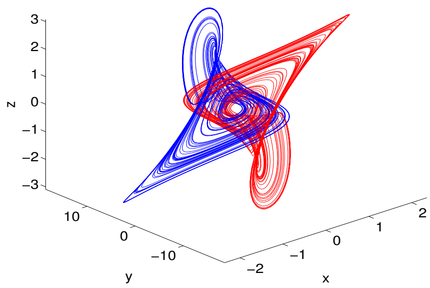

(**b**)

Figure 10. (**a**) The red plot corresponds to system (11), and the blue plot corresponds to system (12), with (a,b,c,d)=(1,22,16,10). (**b**) The red plot corresponds to system (13), and the blue plot corresponds to system (1), with $(a, b, c, d) = (0.4, 50, 16, 10)$.

In addition, if we only revise $C = (1, -1, -1)^T$ in system (8), system (13) is chaotic for the same parameters as system (1), when we have the parameters $a = 0.4, b = 50, c = 16,$

and $d = 10$ and the initial value $(0.1, 0.1, 0.1)^T$. The two chaotic attractors are shown in Figure 10b.

$$\begin{cases} \dot{x} = ay + yz, \\ \dot{y} = -bz - xz, \\ \dot{z} = cx - xy - dz. \end{cases} \tag{13}$$

5. Electronic Circuit Design

In this section, we present an equivalent electronic circuit for the proposed chaotic system (1). The circuit implementation shows that it can be practically used in technological applications. In order to implement the equations, we considered the analog circuit design using Multisim software, as depicted in Figure 11, with AD712KN operational amplifiers and AD633 analog multipliers all powered by ±15 V symmetric voltages.

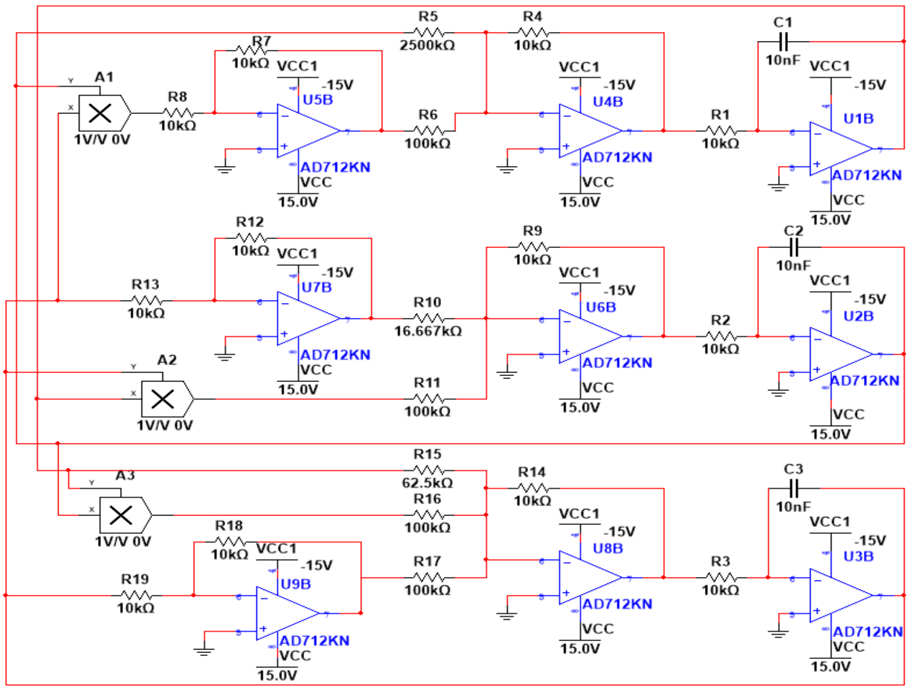

Figure 11. Electronic circuit schematics of the chaotic system (1).

Using the Kirchhoff Law for the analog circuit, the generated nonlinear equations are described as

$$\begin{cases} \dot{x} = \frac{R_4}{R_1 R_5 C_1} y + \frac{R_4 R_7}{R_1 R_6 R_8 C_1} yz, \\ \dot{y} = -\frac{R_9 R_{12}}{R_2 R_{10} R_{13} C_2} z + \frac{R_9}{R_2 R_{11} C_2} zx, \\ \dot{z} = \frac{R_{14}}{R_3 R_{15} C_3} x + \frac{R_{14}}{R_3 R_{16} C_3} xy - \frac{R_{14} R_{18}}{R_3 R_{17} C_3} z. \end{cases} \tag{14}$$

Comparing Equation (14) with Equation (1), the common circuital component values were selected as $C_1 = C_2 = C_3 = 10$ nF, $R_i = 10$ kΩ $(i = 1, 2, 3, 4, 9, 14)$, $R_i = 100$ kΩ $(i = 6, 11, 16)$, and $R_i = 10$ kΩ $(i = 7, 8, 12, 13, 18, 19)$. When we chose $R_5 = 2500$ kΩ, $R_{10} = 16.67$ kΩ, $R_{15} = 62.5$ kΩ, and $R_{17} = 100$ kΩ, we obtained a one-scoll chaotic attractor similar to the one obtained by numerical simulation with $(a, b, c, d) = (0.4, 60, 16, 10)$, and the Multisim results on oscilloscope are shown as Figure 12a,b. When we chose $R_5 = 200$ kΩ, $R_{10} = 20$ kΩ, $R_{15} = 166.67$ kΩ, and $R_{17} = 76.92$ kΩ, and modified the connection R_{15} to R_1, we obtained a two-scoll chaotic attractor similar to the one obtained by numerical simulation with $(a, b, c, d) = (5, 50, -6, 13)$, and the Multisim results on the oscilloscope are shown as Figure 12c,d.

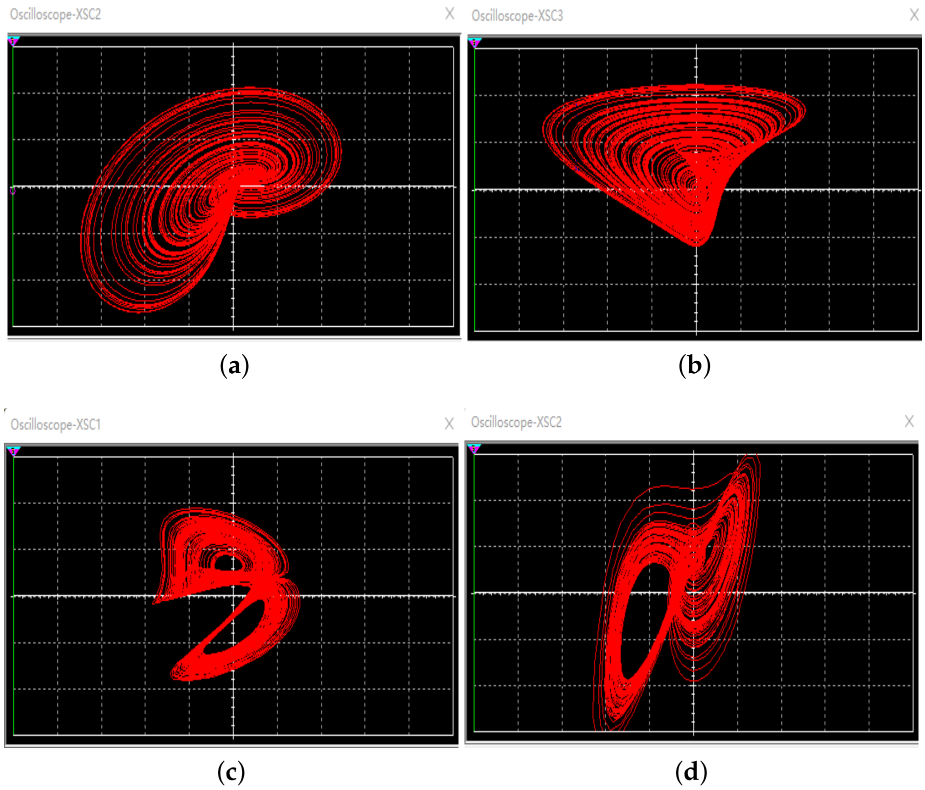

Figure 12. Phase spaces of the chaotic system (1) on an oscilloscope obtained from the analog circuit: (**a**) x-z; (**b**) y-z; (**c**) x-z; (**d**) y-z.

6. Parameter Identification

In this section, we supposed that the parameters a, b, c, and d of system (1) were unknown and needed to be identified. We regarded system (1) as the drive system. The response system with adaptive controllers and updating laws was designed as:

$$\begin{cases} \dot{x_1} = a_1 y_1 - y_1 z_1 + u_1, \\ \dot{y_1} = -b_1 z_1 + z_1 x_1 + u_2, \\ \dot{z_1} = c_1 x_1 + x_1 y_1 - d_1 z_1 + u_3, \end{cases} \tag{15}$$

where a_1, b_1, c_1, and d_1 were the estimations of a, b, c, and d, and u_1, u_2, and u_3 were controllers to be designed.

Theorem 1. *If we design the controllers u_1, u_2, and u_3 in (15) as*

$$\begin{cases} u_1 = -k_1 e_x, \\ u_2 = -k_2 e_y - x_1 e_z, \\ u_3 = -k_3 e_z - x e_y, \\ \dot{k}_1 = \alpha_1 e_x^2, \\ \dot{k}_2 = \alpha_2 e_y^2, \\ \dot{k}_3 = \alpha_3 e_z^2, \end{cases} \tag{16}$$

where α_1, α_2, and α_3 are positive constants, and the updating laws of a_1, b_1, c_1, and d_1 as

$$\begin{cases} \dot{a}_1 = -\theta_1 y_1 e_x, \\ \dot{b}_1 = \theta_2 z_1 e_y, \\ \dot{c}_1 = -\theta_3 x_1 e_z, \\ \dot{d}_1 = \theta_4 z_1 e_z, \end{cases} \tag{17}$$

where $\theta_1,\ \theta_2,\ \theta_3$, and θ_4 are positive constants, then the adaptive synchronization between the drive–response systems (1) and (15) is achieved, and the unknown parameters $a,\ b,\ c$, and d in (1) are identified by $a_1,\ b_1,\ c_1$, and d_1 in (15), with controllers (16) and updating laws (17).

Proof. Let $e_x = x_1 - x, e_y = y_1 - y$, and $e_z = z_1 - z$; then, one has

$$\begin{cases} \dot{e_x} = (a_1 - a)y_1 + ae_y - y_1 e_z - e_y z + u_1, \\ \dot{e_y} = -(b_1 - b)z_1 - be_z + x_1 e_z + e_x z + u_2, \\ \dot{e_z} = (c_1 - c)x_1 + ce_x + e_x y_1 + xe_y - (d_1 - d)z_1 - de_z + u_3. \end{cases} \tag{18}$$

We consider the following Lyapunov function

$$\begin{aligned} V(t) =& \frac{e_x^2 + e_y^2 + e_z^2}{2} + \frac{(a_1 - a)^2}{2\theta_1} + \frac{(b_1 - b)^2}{2\theta_2} \\ &+ \frac{(c_1 - c)^2}{2\theta_3} + \frac{(d_1 - d)^2}{2\theta_4} + \sum_{i=1}^{3} \frac{(k_i - k_i^*)^2}{2\alpha_i}, \end{aligned} \tag{19}$$

where $k_1^*,\ k_2^*$, and k_3^* are arbitrary positive constants to be determined.

Then, the derivative of $V(t)$ along the trajectories of (18) gives

$$\begin{aligned} \dot{V}(t) =& e_x\dot{e}_x + e_y\dot{e}_y + e_z\dot{e}_z + \frac{(a_1 - a)\dot{a}_1}{\theta_1} + \frac{(b_1 - b)\dot{b}_1}{\theta_2} \\ &+ \frac{(c_1 - c)\dot{c}_1}{\theta_3} + \frac{(d_1 - d)\dot{d}_1}{\theta_4} + \sum_{i=1}^{3} \frac{(k_i - k_i^*)\dot{k}_i}{\alpha_i} \\ =& e^T(P - K)e, \end{aligned}$$

where $e = (e_x, e_y, e_z)^T$,

$$P = \begin{pmatrix} 0 & \frac{a}{2} & \frac{c}{2} \\ \frac{a}{2} & 0 & -\frac{b}{2} \\ \frac{c}{2} & -\frac{b}{2} & -d \end{pmatrix},\ K = \begin{pmatrix} k_1^* & 0 & 0 \\ 0 & k_2^* & 0 \\ 0 & 0 & k_3^* \end{pmatrix}.$$

Then, one can choose $k_1^*,\ k_2^*$, and k_3^* large enough such that $P - K < 0$, i.e., $\dot{V}(t) < 0$, which implies that the adaptive synchronization is achieved, and the unknown parameters $a,\ b,\ c$, and d are identified by $a_1,\ b_1,\ c_1$, and d_1. Thus, the proof is complete. □

In the simulations, we designed the corresponding electronic circuit with controllers (16) and updating laws (17) to identify the unknown parameters using Multisim software. Figure 13 shows the electronic circuit design with the AD712KN operational amplifiers and AD633 analog multipliers all powered by ± 15 V symmetric voltages. We supposed that the resistances R_{22}, R_{12}, R_{14}, and R_{17} of the drive system corresponding to the parameters $a = 0.4,\ b = 60,\ c = 16$, and $d = 10$ of system (1) were unknown and needed to be identified. We chose the following resistances of the updating laws $R_a = R_b = R_c = R_d = 50\ \text{k}\Omega$ and the following resistances of the controllers $R_{K_1} = R_{K_2} = R_{K_3} = 100\ \text{k}\Omega$. The Multisim results on the oscilloscope are shown as Figure 14a,b. Clearly, the unknown parameters $a,\ b,\ c$, and d were well identified by $a_1,\ b_1,\ c_1$, and d_1.

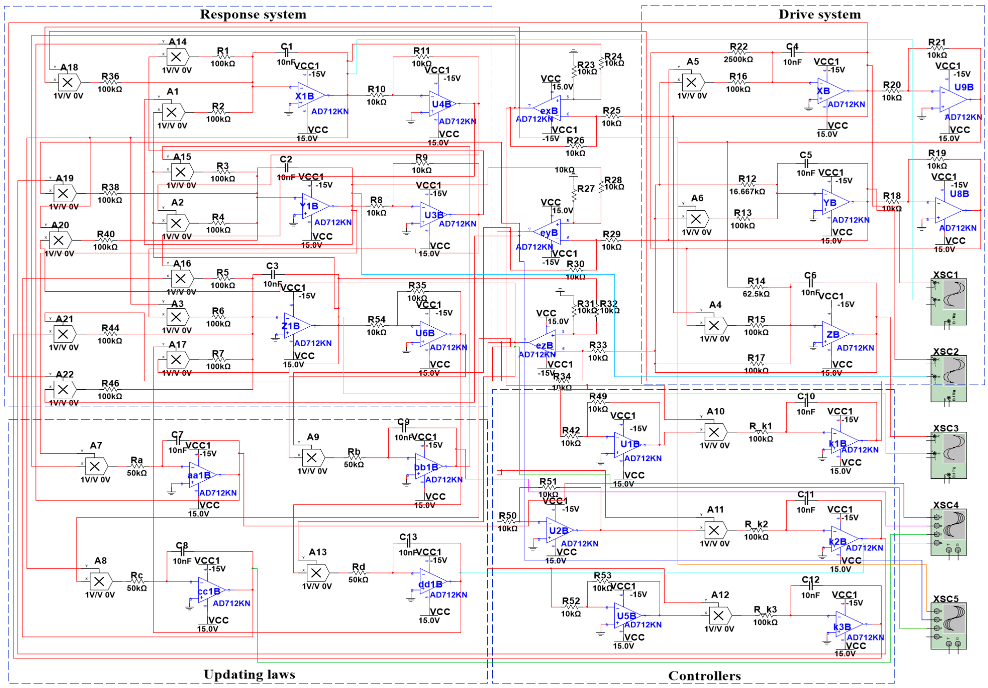

Figure 13. Electronic circuit schematics of the parameter identification.

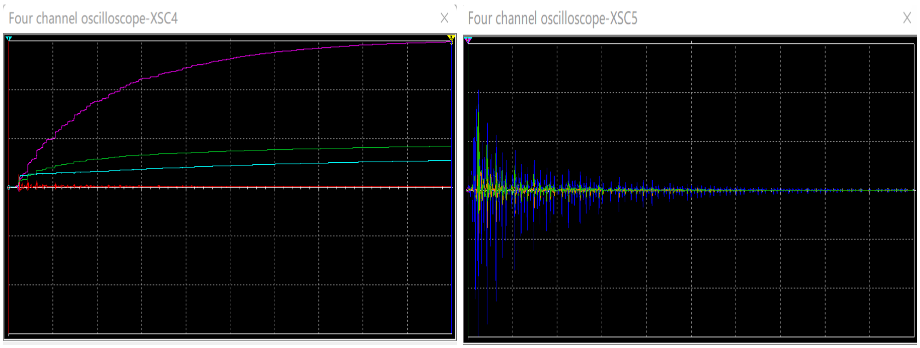

(**a**) (**b**)

Figure 14. Identification of a_1, b_1, c_1, and d_1 by an electronic circuit.

7. Conclusions

In this paper, we introduced and studied a new 3D autonomous chaotic system, which could generate one-scroll and two-scroll chaotic attractors with different parameters. The dynamical behaviors and properties of this chaotic system were investigated both theoretically and numerically. The Lyapunov exponent spectrum and the corresponding bifurcation diagram, with respect to different parameters, were presented, and these validated the correctness of our results. Spectral analysis showed that the system had a large chaos region. Moreover, a vector map was employed to the generalized chaotic system. Compared with the famous Rössler, Sprott, and Lorenz attractors, this system is a supplement to the discovery of one-scroll and two-scroll attractors. Further, we designed an equivalent electronic circuit for the proposed chaotic system based on Kirchhoff's Law to show its practical applications. We designed a corresponding response electronic circuit to identify the unknown parameters or monitor the changes in the system parameters as well. Finally, numerical simulations were presented to perform and complement the theoretical results.

Author Contributions: M.L. wrote the original draft, Z.W. and X.F. reviewed and edited the paper. All authors have read and agreed to the published version of the manuscript.

Funding: This work was jointly supported by the scientific research project of the Education Department of Zhejiang Province (No.Y202044362) and the NSFC (No. 61963019).

Institutional Review Board Statement: Not applicable.

Informed Consent Statement: Not applicable.

Data Availability Statement: The data are presented in the manuscript.

Conflicts of Interest: The authors declare no conflict of interest.

References

1. Lorenz, E.N. Deterministic Nonperiodic Flow. *J. Atmos. Sci.* **1963**, *20*, 130–141. . [CrossRef]
2. Fallahi, K.; Leung, H. A chaos secure communication scheme based on multiplication modulation. *Commun. Nonlinear Sci. Numer. Simul.* **2010**, *15*, 368–383. . [CrossRef]
3. Rössler, O.E. An equation for continuous chaos. *Phys. Lett. A* **1976**, *57*, 397–398. . [CrossRef]
4. Chen, G.; Ueta, T. Yet another chaotic attractor. *Int. J. Bifurc. Chaos* **1999**, *9*, 1465–1466. . [CrossRef]
5. Lü, J.; Chen, G.; Cheng, D.; Celikovsky, S. Bridge the gap between the Lorenz system and the Chen system. *Int. J. Bifurc. Chaos Appl. Sci. Eng.* **2002**, *12*, 2917–2926. . [CrossRef]
6. Liu, W.; Chen, G. A new chaotic system and its generation. *Int. J. Bifurc. Chaos Appl. Sci. Eng.* **2003**, *13*, 261–267. . [CrossRef]
7. Lü, J.; Chen, G.; Cheng, D. A New Chaotic System and Beyond: The Generalized Lorenz-like System. *Int. J. Bifurc. Chaos* **2004**, *14*, 1507–1537. [CrossRef]
8. Dong, G.; Du, R.; Tian, L.; Jia, Q. A novel 3D autonomous system with different multilayer chaotic attractors. *Phys. Lett. Sect. A: Gen. At. Solid State Phys.* **2009**, *373*, 3838–3845. . [CrossRef]
9. Wang, Z.; Qi, G.; Sun, Y.; Van Wyk, B.J.; Van Wyk, M.A. A new type of four-wing chaotic attractors in 3-D quadratic autonomous systems. *Nonlinear Dyn.* **2010**, *60*, 443–457. . [CrossRef]
10. Wei, Z.; Yang, Q. Dynamical analysis of a new autonomous 3-D chaotic system only with stable equilibria. *Nonlinear Anal. Real World Appl.* **2011**, *12*, 106–118. . [CrossRef]
11. Liu, Y. Analysis of global dynamics in an unusual 3D chaotic system. *Nonlinear Dyn.* **2012**, *70*, 2203–2212. [CrossRef]
12. Wang, X.; Chen, G. Constructing a chaotic system with any number of equilibria. *Nonlinear Dyn.* **2013**, *71*, 429–436. . [CrossRef]
13. Li, C.; Sprott, J.C.; Xing, H. Constructing chaotic systems with conditional symmetry. *Nonlinear Dyn.* **2017**, *87*, 1351–1358. . [CrossRef]
14. Wang, G.; Yuan, F.; Chen, G.; Zhang, Y. Coexisting multiple attractors and riddled basins of a memristive system. *Chaos* **2018**, *28*, 013125. . [CrossRef]
15. Zhang, X.; Wang, C.; Yao, W.; Lin, H. Chaotic system with bondorbital attractors. *Nonlinear Dyn.* **2019**, *97*, 2159–2174. . [CrossRef]
16. Xie, Q.; Zeng, Y. Generating different types of multi-double-scroll and multi-double-wing hidden attractors. *Eur. Phys. J. Spec. Top.* **2020**, *229*, 1361–1371. . [CrossRef]
17. Gong, L.; Wu, R.; Zhou, N. A New 4D Chaotic System with Coexisting Hidden Chaotic Attractors. *Int. J. Bifurc. Chaos* **2020**, *30*, 2050142. . [CrossRef]
18. Zhou, L.; You, Z.; Tang, Y. A new chaotic system with nested coexisting multiple attractors and riddled basins. *Chaos Solitons Fractals* **2021**, *148*, 111057. . [CrossRef]
19. Ma, C.; Mou, J.; Xiong, L.; Banerjee, S.; Liu, T.; Han, X. Dynamical analysis of a new chaotic system: Asymmetric multistability, offset boosting control and circuit realization. *Nonlinear Dyn.* **2021**, *103*, 2867–2880. . [CrossRef]
20. Wang, R.; Li, C.; Kong, S.; Jiang, Y.; Lei, T. A 3D memristive chaotic system with conditional symmetry. *Chaos Soliton Fractal* **2022**, *158*, 111992. [CrossRef]
21. Vanecek, A., Celikoshy, S. *Control Systems: From Linear Analysis to Synthesis of Chaos*; Prentice-Hall: London, UK, 1996.
22. Sprott, J.C. Some simple chaotic flows. *Phys. Rev. E* **1994**, *50*, R647–R650. . [CrossRef] [PubMed]
23. Sprott, J.C. Simplest dissipative chaotic flow. *Phys. Lett. Sect. A: Gen. At. Solid State Phys.* **1997**, *228*, 271–274. . [CrossRef]
24. Huang, K.; Yang, Q. Stability and Hopf bifurcation analysis of a new system. *Chaos Solitons Fractals* **2009**, *39*, 567–578. . [CrossRef]
25. Zheng, S.; Dong, G.; Bi, Q. A new hyperchaotic system and its synchronization. *Appl. Math. Comput.* **2010**, *215*, 3192–3200. . [CrossRef]
26. Wolf, A.; Swift, J.B.; Swinney, H.L.; Vastano, J.A. Determining Lyapunov exponents from a time series. *Phys. D: Nonlinear Phenom.* **1985**, *16*, 285–317. . [CrossRef]